Spred1, a negative regulator of Ras–MAPK–ERK, is enriched in CNS germinal zones, dampens NSC proliferation, and maintains ventricular zone structure

Timothy N. Phoenix and Sally Temple[1]

New York Neural Stem Cell Institute, Rensselaer, New York 12144, USA; and Center for Neuropharmacology and Neuroscience, Albany Medical College, Albany, New York 12208, USA

Neural stem cells (NSCs) have great potential for self-renewal, which must be tightly regulated to generate appropriate cell numbers during development and to prevent tumor formation. The Ras–MAPK–ERK pathway affects mitogen-stimulated proliferation, and negative regulators are likely to be important for keeping self-renewal in check. Sprouty-related protein with an EVH1 domain (Spred1) is a recently discovered negative Ras–MAPK–ERK regulator linked to a neurofibromatosis 1 (NF-1)-like human syndrome; however, its role in CNS development has not been explored. We show that *Spred1* is highly enriched in CNS germinal zones during neurogenesis. Spred1 knockdown increases NSC self-renewal and progenitor proliferation cell-autonomously, and overexpression causes premature differentiation. Surprisingly, Spred1 knockdown in vivo in the embryonic mouse forebrain frequently resulted in periventricular heterotopia, developmental abnormalities often associated with mutations in genes in the vesicular trafficking pathway that cause disruption of germinal zones and impair cell migration. In cortical progenitor cells, Spred1 localizes within distinct vesicles, indicating a potential role in transport. Spred1 knockdown gradually leads to disruption of the apical ventricular zone and loss of radial glia alignment. This impairs late neuronal migration, resulting in the formation of periventricular masses. Thus, Spred1 is critical for normal cortical development, as it modulates progenitor self-renewal/proliferation and helps maintain the integrity and organization of germinal zones.

[*Keywords*: Spred1; neural stem cells; self-renewal; MAPK–ERK signaling; periventricular heterotopia]

Supplemental material is available at http://www.genesdev.org.

Received July 3, 2009; revised version accepted November 9, 2009.

In the developing CNS, neural stem cells (NSCs) and neural progenitor cells (NPCs) self-renew and proliferate to create a founder cell population, which then begins to generate differentiated progeny: first, neurons during the embryonic period, and then glia, largely postnatally (Bayer et al. 1991; Miller and Gauthier 2007). A number of exogenous growth factors and cytokines have been identified that modulate the balance of CNS progenitor proliferation and differentiation, many of them revealed using development of the cerebral cortex as a model system. Mitogens such as FGF2, EGF, and VEGF stimulate cortical progenitor cell division (Burrows et al. 1997; Vaccarino et al. 1999; Jin et al. 2002), while factors such as bone morphogenetic protein (BMP), ciliary neurotrophic factor (CNTF), and Cardiotrophin-1 can induce premature cortical gliogenesis (Barnabe-Heider and Miller 2003; Barnabe-Heider et al. 2005). Many of these factors converge on the Ras–MAPK–ERK signaling pathway, which integrates inputs to alter the duration and intensity of the receptor-mediated signals, and thus effects progenitor cell behavior (Miller and Gauthier 2007).

Multiple developmental disorders are associated with hyperactive Ras signaling, including neurofibromatosis 1 (NF1) and Noonan syndrome, which affect ~1:3000 and 1:2500 individuals in the United States, respectively (Noonan 1994; Cichowski and Jacks 2001; Zhu and Parada 2001). Besides presenting with common tumor phenotypes and skin/skeletal abnormalities, these disorders are highly associated with macrocephaly, learning disabilities, mental retardation, and autism (Mbarek et al. 1999; Costa et al. 2002; Marui et al. 2004; Schubbert et al. 2007). Although some of the CNS defects are due to the important role of Ras signaling in learning and plasticity (Cui et al. 2008), patients can also exhibit developmental

[1]**Corresponding author.**
E-MAIL sallytemple@nynsci.org; FAX (518) 694-8187.
Article is online at http://www.genesdev.org/cgi/doi/10.1101/gad.1839510.

malformations that could contribute to neural impairment—for example, cell heterotopia, cortical lamination defects, and periventricular tumors—indicating a significant function in CNS progenitor cells (Korf et al. 1999; Balestri et al. 2003; Vivarelli et al. 2003; Fedi et al. 2004).

Specific gene products that impact the Ras–MAPK–ERK pathway (notably, *NF1* and *SHP2*) have been identified as main causes (up to 50% of cases) of hyperactive Ras diseases, and more are being sought (Schubbert et al. 2007). Moreover, the mechanism by which these Ras regulatory molecules act to create the observed CNS defects are being elucidated; each has different effects due to its unique action on the Ras pathway and effects on other pathways. For example, loss of SHP2, a positive regulator of the Ras pathway, stimulates gliogenesis and reduces neurogenesis via a decrease in Ras–MAPK signaling and an increase in Jak–Stat signaling (Gauthier et al. 2007). Loss of NF1, a negative regulator of Ras, stimulates forebrain progenitor self-renewal via its action on Ras–MAPK–ERK, but also increases progenitor cell survival by increasing phospho-AKT (p-AKT), and impairs neuronal maturation via an interaction with the cAMP pathway (Dasgupta and Gutmann 2005; Hegedus et al. 2007). Such pleiotropic actions can explain why, for example, loss of NF1 in progenitor populations over the course of development can yield quite different effects (Zhu et al. 2001, 2005; Dasgupta and Gutmann 2005; Hegedus et al. 2007; Lush et al. 2008).

Recently, Sprouty-related protein with an EVH1 (Ena/VASP [vasodilator-stimulated phosphoprotein] homology domain 1) domain (*SPRED1*) was identified as a negative regulator of the Ras–MAPK–ERK pathway (Wakioka et al. 2001). Spred1 protein is normally expressed in various adult organs and tissues, including the brain, and it is highly expressed in the brain during fetal development (Kato et al. 2003; Engelhardt et al. 2004). Loss of SPRED1 function causes an NF1-like phenotype in humans (Brems et al. 2007). Knockout mice have deficits in hippocampal-dependent learning and synaptic plasticity (Brems et al. 2007; Denayer et al. 2008), but the role of Spred proteins in forebrain progenitor cells has not yet been investigated.

Spred1 inhibits the Ras–MAPK–ERK pathway downstream from NF1, at the level of Raf, interacting with its C-terminal catalytic domain (Sasaki et al. 2003; Bundschu et al. 2007). When overexpressed in a highly metastatic mouse osteosarcoma cell line, Spred1 can inhibit RhoA-mediated cell motility and signal transduction (Miyoshi et al. 2004), but its role in neuronal migration has not been examined. In that regard, it has an N-terminal-enabled/VASP domain, and VASP proteins are important for neuron migration (Goh et al. 2002) as well as epithelial junction formation (Lawrence et al. 2002). Hence, we anticipate that Spred-1 might have important functions in the developing CNS, where changes in epithelial structure, cell proliferation, and cell migration must be coordinated to achieve normal development.

Given its association with developing brain and with Ras disorders in humans and mice, we investigated the role of Spred1 in cortical development and its action in cortical progenitor cells. Our data show that Spred1 is an important modulator of Ras–MAPK–ERK signaling in the developing forebrain, influencing the self-renewal and proliferation of multipotent NSCs and NPCs. Furthermore, we suggest that its ability to interact with intracellular vesicular trafficking can produce developmental forebrain abnormalities such as periventricular heterotopia (PVH).

Results

Spred1 is specifically expressed in the ventricular zone (VZ) and subventricular zone (SVZ) during cortical development

We performed in situ hybridization for *Spred1* on cryostat sections of developing mouse brains, focusing on the cerebral cortex. At embryonic day 11.5 (E11.5), when the cortex consists largely of dividing progenitor cells that reside in the VZ, *Spred1* is expressed throughout the VZ, with the strongest expression near the apical edge where the principle progenitor cells reside, becoming more scattered toward the basal aspect of the VZ (Fig. 1A; Supplemental Fig. 1A). *Spred1* is also highly expressed in the midline anterior commissural plate, where FGF8 is secreted (Fig. 1A). The related Sprouty 1 protein is similarly expressed in this midline location, but is largely absent from the developing cortex (data not shown). As neurogenesis progresses, midline expression of *Spred1* disappears, and by midgestation, around E14, it becomes largely restricted to the cortical VZ and the secondary germinal layer, the SVZ. At E17, which marks the late

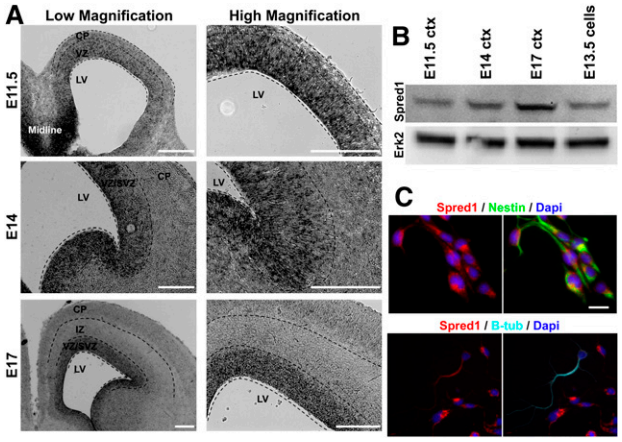

Figure 1. Expression of *Spred1* mRNA and protein in the developing cerebral cortex. (*A*) In situ hybridization for *Spred1* mRNA in coronal sections of mouse cerebral cortex. E11.5 *Spred1* mRNA is highly expressed in midline structures, and is scattered throughout progenitor cells in the cortical VZ. E14 *Spred1* expression is restricted mainly to the VZ/SVZ germinal zones. E17 *Spred1* expression is maintained in the VZ/SVZ, with weak expression in the cortical plate. (LV) Lateral ventricle; (IZ) intermediate zone; (CP) cortical plate. (*B*) Western blot for Spred1 protein in cortical homogenates. Erk2 Western blot for protein loading control. (*C*) Immunocytochemistry for Spred1 in E13.5 cortical culture. The *top* panels show Spred1 staining (red) in Nestin$^+$ (green) precursors. The *bottom* panels show Spred1 staining with the neuronal marker β-Tubulin III (light blue). Bars: *A*, 200 μm; *C*, 50 μm.

stages of neurogenesis and the beginning of gliogenesis in the cortex, Spred1 is still expressed in the VZ/SVZ—again, with strongest expression in the VZ, and weaker expression detected in differentiated neurons located in the cortical plate and hippocampus (Fig. 1A; Supplemental Fig. 1A).

To verify translation, we used freshly isolated cortical protein homogenates to identify Spred1 protein expression in the developing cortex. At all stages analyzed (E11.5, E13.5, and E17), we detected a band of the appropriate size (~50 kDa) of Spred1 protein (Fig. 1B). Protein samples from E11.5 and E13.5 neurospheres that were cultured for 7 d in vitro (DIV) also showed expression of Spred1 (Fig. 1B; data not shown). We performed immunocytochemistry on E13.5 cortical progenitors that were cultured for 3 DIV. Spred1 was expressed in Nestin$^+$ progenitor cells in a punctate staining pattern in the cytoplasm (Fig. 1C), and weakly labeled some β-tubulin III$^+$ immature neurons (Fig. 1C, bottom panels). To further investigate the subcellular localization, we colabeled E11.5 cells at 3 DIV with Spred1 and Rab5 or Rab11 antibodies. Spred1 colocalized extensively with Rab5, which is associated with early endosome vesicles (Supplemental Fig. 2A), and to a lesser extent with Rab11, which is a late endosomal vesicle marker (Supplemental Fig. 2B). Thus, Spred1 appears to be associated with different lipid membrane vesicles with various functions, including endocytosis, vesicle trafficking, and exocytosis. Based on its distribution, Spred-1 is likely to preferentially impact Ras–MAPK–ERK signaling in progenitor cell populations during forebrain development.

Spred1 inhibits Ras–MAPK–ERK activity and self-renewal/proliferation of cortical progenitor cells

We examined Spred-1 function in isolated embryonic cortical cells using acute knockdown with lentiviral vector-delivered shRNA constructs. Three different lentiviral constructs (Spred1 shRNA1–3; two targeting the ORF, and one targeting the 3′ [untranslated region] UTR) each significantly decreased *Spred1* mRNA levels to 25%–40% of control vector levels, resulting in notable reduction in Spred1 protein (decreased to 30%–50% of control levels) as assessed by Western blot (Fig. 2A,B). Since Spred1 has been shown to modulate the Ras–MAPK–ERK pathway, we examined phosphorylated ERK (p-ERK) levels in neurosphere cultures that originated from E11.5 progenitor cells transduced with either empty vector (EV) control or shRNA constructs. After 1 wk in culture, the resulting neurospheres were starved overnight and then harvested. Compared with EV control, cultures transduced with Spred1 shRNA constructs displayed an approximately threefold increase in p-ERK levels (Fig. 2A). We also assayed for levels of p-AKT, an important signaling pathway for cell survival, but did not detect any robust changes. Thus, Spred1 shRNA treatment specifically decreased *Spred1* mRNA and protein levels, resulting in enhanced Ras–MAPK–ERK signaling activity.

We then asked whether reducing Spred1 would alter progenitor behavior. Isolated E11.5 cortical cells were treated with shRNA or EV control constructs, achieving >95% cell transduction. Single cells were plated in serum-free medium containing 10 ng/mL mitogen FGF2. After 3 DIV, clones were immunostained for activated caspase 3 to assess survival, for Ki67 to assess proliferation, and for β-tubulin III for neuronal differentiation. Cultures transduced with Spred1 shRNA constructs did not show a difference in cell death (EV control = 27.4% ± 1.9%; Spred1 shRNA = 26.6% ± 3.1%) (Fig. 2B), but displayed a significant increase in proliferating Ki67$^+$ cells per clone (EV control = 60.2% ± 3.8%; Spred1 shRNA = 86.2% ± 1.8%) (Fig. 2C), and a corresponding decrease in the proportion of differentiated β-tubulin III$^+$ neurons. After 6 DIV, Spred1 shRNA clones were larger and still contained more Nestin$^+$ progenitor cells and fewer neurons than controls (Fig. 2D–F). The fact that this occurs in clonal culture demonstrates that Spred1 reduction acts cell-autonomously to stimulate progenitor cell division.

In order to assess whether Spred1 knockdown affected proliferation of subtypes of progenitor cells, we stained the cultures for Pax6 and Tbr2, which label apical and basal progenitors, respectively. In E11 cortical cultures at 6 DIV, Spred1 shRNA treatment produced a significant increase in Pax6$^+$ cells (EV control = 41.1% ± 2.9%; Spred1 shRNA = 54.5% ± 3.7%) (Fig. 2F), and a smaller but significant decrease in Tbr2$^+$ cells (EV control = 11.1% ± 1.6%; Spred1 shRNA = 5.6% ± 1.2%) (Fig. 2F). These data suggest that Spred1 knockdown impacts mainly proliferation of apical radial glia progenitor cells, rather than the more basal intermediate progenitors.

Given prior data indicating that Spred1 acts as a MEK inhibitor, we tested this directly in the NPC population. Cortical progenitor cells transduced with Spred1 shRNA or with EV control vector were treated with the known MEK inhibitor PD98059 for 3 DIV. This eliminated the proliferative effect of shRNA treatment described above (using Ki67 staining to indicate proliferation; EV control = 42.1% ± 3.5%; Spred1 shRNA = 44.2% ± 3.3%), demonstrating that Spred1 functions as a specific inhibitor of MAPK–ERK signaling in cortical NPCs (Supplemental Fig. 3B).

Next, we used the neurosphere assay to ask whether Spred1 impacts self-renewal. Isolated E14 cortical progenitor cells were transduced with Spred1 shRNA versus EV control constructs as described, and were cultured in nonadherent conditions in the presence of FGF2 and EGF, allowing stem and progenitor cells that are responsive to these mitogens to divide and form floating multicell neurospheres. After 1 wk, cultures that received Spred1 shRNA constructs produced 25%–40% more primary neurospheres compared with EV control. Upon passaging, the Spred1-transduced neurospheres produced ~40% more secondary spheres, indicating that self-renewal is stimulated (Fig. 3B,C). These data further support the results obtained using adherent culture assays, indicating that Spred1 inhibits cortical progenitor self-renewal and proliferation, even in the presence of added exogenous mitogens, through its ability to inhibit the Ras–MAPK–ERK pathway.

To see if enforced expression of Spred1 would result in the opposite phenotype, we used a Spred1 overexpression

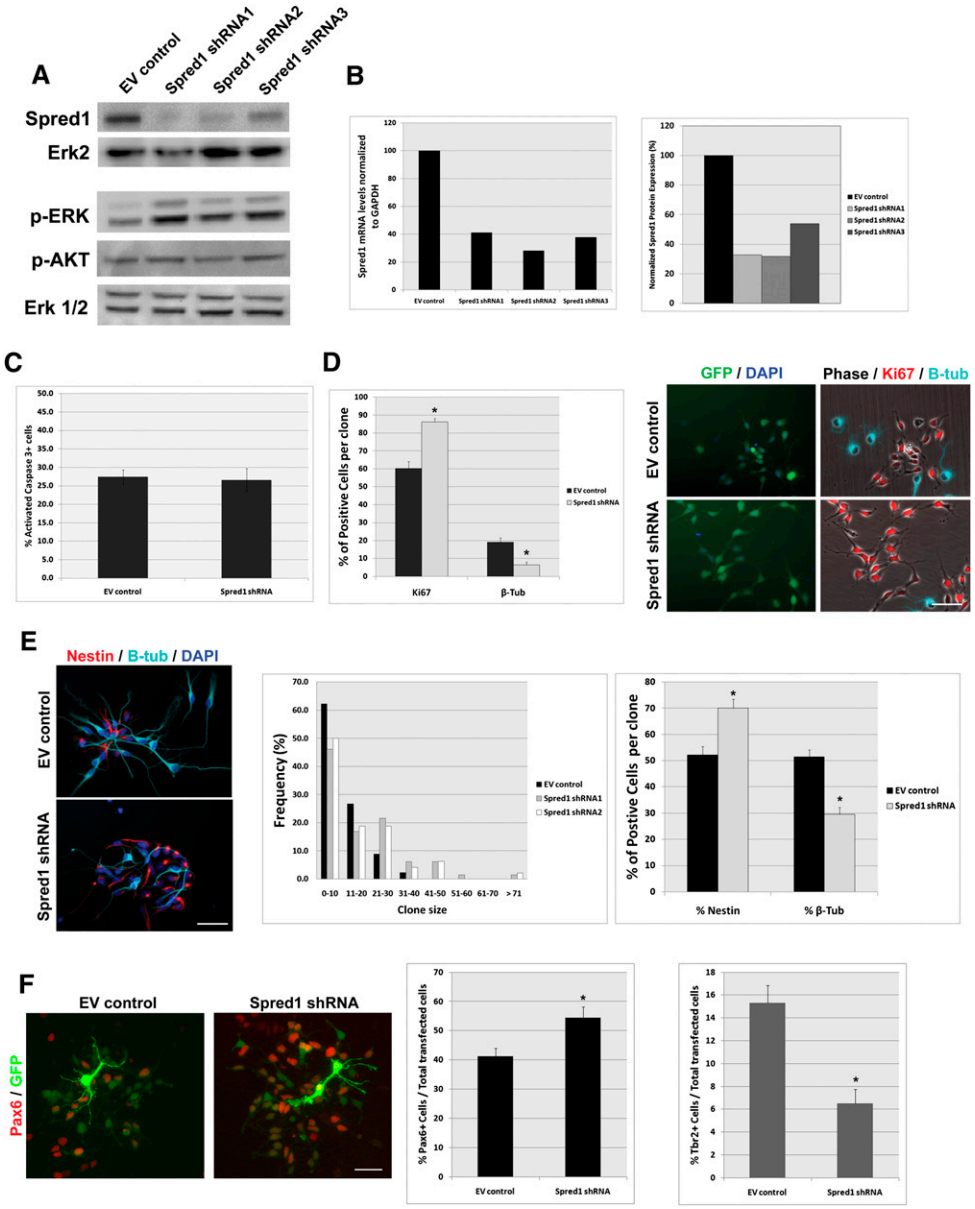

Figure 2. shRNA Spred1 treatment of E11.5 cortical cells increases p-ERK levels and enhances progenitor self-renewal and proliferation. (*A*) Western blot for Spred1, p-ERK, p-AKT, ERK, and total ERK levels after shRNA transduction. (*B*) *Spred1* mRNA levels after Spred1 shRNA transduction in E11.5 cortical cultures, and quantification of Spred1 protein levels from Western blots (in the *right* panel, NIH Image J was used to quantify densities). (*C*) Quantification of activated Caspase 3 in E11.5 cortical progenitors at 3 DIV (n = 2, t-test, $P > 0.05$). (*D*) E11.5 cortical cells transduced with Spred1 shRNA displayed a significant increase in the percentage of proliferating Ki67$^+$ cells within clones (n = 3, t-test, [*] $P < 0.005$) and decrease in the percentage of β-tubulin III$^+$ neurons per clone (n = 3, t-test, [*] $P < 0.005$) after 3 DIV. (*E*) After 6 DIV, E11.5 cortical cells transduced with Spred1 shRNA constructs displayed an increase in clone size frequency, an increase in the percentage of cells labeled with the progenitor marker Nestin per clone (n = 2, t-test, [*] $P <$ 0.005), and a decrease in the percentage of β-tubulin III$^+$ neurons per clone (n = 2, [*] $P < 0.005$). (*F*) Spred1 shRNA-transfected E11.5 cortical cultures after 6 DIV display an increase in Pax6$^+$/GFP$^+$ cells (n = 2, t-test, [*] $P < 0.05$), and a decrease in Tbr2$^+$/GFP$^+$ cells (n = 2, t-test, [*] $P < 0.005$). Bars: *D–F*, 50 μm. Error bars represent SEM.

construct. E11.5 cortical progenitors were transfected with EV control, shRNA, or overexpression plasmids and fixed after 3 DIV. Spred1 overexpression significantly decreased proliferation, indicated by Ki67$^+$ staining (EV control = 37.3% ± 3.9%; Spred1 overexpression = 21.9% ± 3.1%), and most transduced cells had differentiated into post-mitotic neurons (EV control = 60.7% ± 3.2%; Spred1 overepression = 78.0% ± 3.9%) (Fig. 3A). Even in the presence of the MEK inhibitor, overexpression of Spred1 decreased progenitor proliferation, suggesting that it is a stronger inhibitor (Supplemental Fig 3B). Consistent with these findings, primary neurosphere formation was

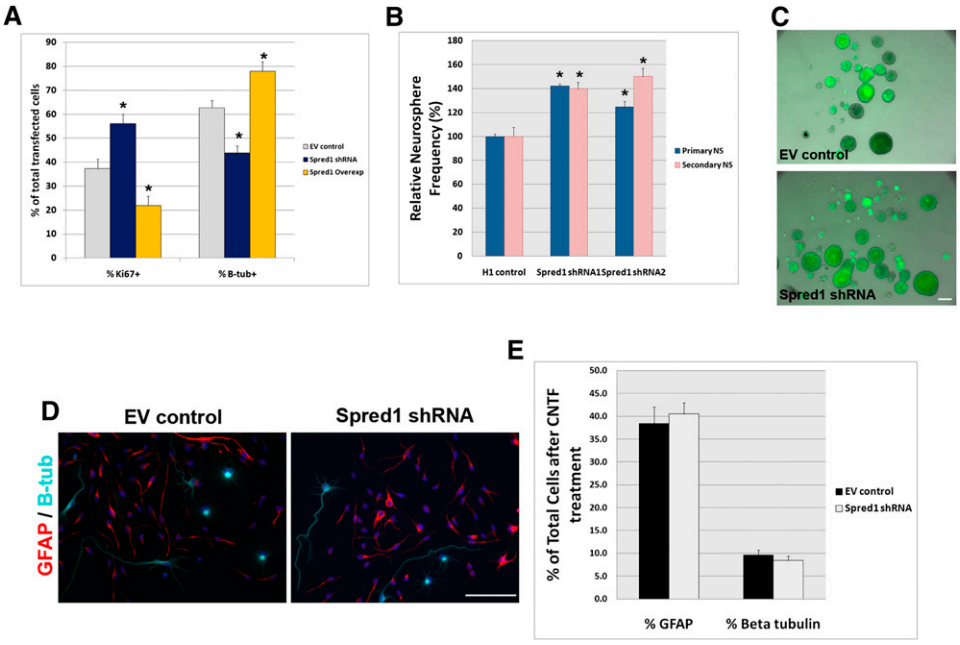

Figure 3. Knockdown of Spred1 increases formation of neurospheres but does not alter fate decisions, and overexpression of Spred1 results in progenitor differentiation. (*A*) Transfection of Spred1 overexpression construct results in decreased progenitor proliferation (Ki67) and increased differentiation (B-tub) at 3 DIV (Ki67 and B-tub; ANOVA, [*] $P < 0.01$ significant Bonferroni post-hoc test). (*B*) Decreasing Spred1 levels significantly increase the number of both primary and secondary neurospheres compared with EV control transduction (primary NS, ANOVA $P < 0.005$; secondary NS, [*] $P < 0.01$ significant Bonferroni Post-hoc test). (*C*) Representative images of primary EV control and Spred1 shRNA neurospheres. (*D*) E14 cortical cells treated with CNTF for 4 DIV and then stained for GFAP (red) and β-tubulin III (light blue). (*E*) Quantification of GFAP- and β-tubulin III-expressing cells after CNTF treatment reveals no significant difference between EV control and Spred1 shRNA treatment (percentage GFAP, *t*-test, $P > 0.5$; percentage B-tub, *t*-test, $P > 0.5$). Bars: *C*,*D*, 100 μm. Error bars represent SEM.

significantly decreased after Spred1 overexpression compared with mock or EV control (normalized to mock = 100% ± 2.2%; EV control = 102% ± 4.3%; Spred1 overexpression = 60.0% ± 3.7%) (Supplemental Fig. 3A). Thus, overexpression of Spred1 in vitro results in decreased progenitor self-renewal and proliferation and increased differentiation.

Decreasing Spred1 does not impact the early neuron/glial fate choice

Previous studies have shown that levels of MAPK–ERK and Jak–Stat can determine CNS and, specifically, cortical cell fate decisions. Reduction of MAPK–ERK signaling promotes progenitor cells to differentiate, while high levels of Jak–Stat stimulate gliogenesis and reduce neurogenesis (Barnabe-Heider et al. 2005; Gauthier et al. 2007). SHP2 influences both signaling pathways, and therefore modulates both proliferation and neuro/gliogenesis. Given previous evidence that Spred1 does not interact with the Jak–Stat pathway (Nonami et al. 2004), we did not expect Spred1 knockdown to affect the early neuron–glial fate choice. However, we tested this directly by examining whether Spred1 knockdown would impair the capacity of embryonic cortical progenitor cells to make astrocytes.

We cultured E14 cortical progenitor cells in adherent conditions with 10 ng/mL FGF2 for 2 DIV, and then added 50 ng/mL CNTF, which up-regulates Jak–Stat signaling to induce progenitor differentiation and astrocyte production. After 4 DIV exposure to CNTF, cells were fixed and immunostained for GFAP (an astrocyte lineage marker) and β-tubulin III (a neuronal marker). Both EV control and Spred1 shRNA-transduced cultures produced a similar proportion of astrocytes (EV control = 38.4% ± 3.7%; Spred1 shRNA = 40.5% ± 2.4%) and neurons (EV control = 9.6% ± 1.0%; Spred1 shRNA = 8.4% ± 1.0%) (Fig. 3E). Spred1 shRNA-transduced astrocytes and neurons also appeared morphologically normal (Fig. 3D). Thus, while decreasing Spred1 levels clearly increases progenitor self-renewal and proliferation, as seen by an increase in Nestin and Ki67 labeling, it does not notably influence this early cell fate decision. On the other hand, an increase in expression of Spred1 causes embryonic cortical progenitor cells to prematurely differentiate into postmitotic neurons, and we anticipate that the resulting loss of progenitor maintenance would also impair production of the later-born glia progeny. It will be interesting to examine the effect of reducing Spred1 at later stages of development, when the majority of astrocytes and oligodendrocytes are generated.

Spred1 knockdown in utero enhances cortical progenitor proliferation

These in vitro studies enabled precise evaluation of the output of identified progenitor cells after manipulating

Spred1 levels, but do not necessarily reflect the behavior of progenitors in the normal, complex environment of the developing brain. Hence, we performed in utero electroporation to decrease Spred1 expression in embryonic cortical progenitor cells at E14, and harvested tissue for analysis 4 d later at E18. Upon electroporation with EV control plasmid, cells in the VZ/SVZ are transfected and produce differentiated neurons that migrate away from the germinal zone, through the intermediate zone, and into the cortical plate over the next few days. Quantitative analysis of EV control cortices for $GFP^+/Nestin^+$ progenitors (16.5% ± 1.0%) and $GFP^+/\beta\text{-tubulin}^+$ neurons (83.4% ± 0.95%) revealed the distribution of electroporated cells. Embryos in which Spred1 shRNA vector was used had significantly more $GFP^+/Nestin^+$ progenitors (25.5% ± 2.0%) and fewer $GFP^+/\beta\text{-tubulin}^+$ neurons (74.5% ± 2.1%) (Fig. 4A–D). To identify changes in apical or basal progenitor cell behavior, we stained sections for Pax6 and Tbr2. Spred1 knockdown brains had significantly more $GFP^+/Pax6^+$ cells in the VZ/SVZ when compared with EV control (Spred1 shRNA = 52.6% ± 2.8%; EV control = 22.4% ± 1.8%) (Fig. 5A), and fewer $Tbr2^+/GFP^+$ cells in the VZ/SVZ (Spred1 shRNA = 33.2% ± 2.6%; EV control = 55.2% ± 3.0%) (Fig. 5B), further supporting conclusions from in vitro data that decreasing Spred1 preferentially increases apical progenitor self-renewal and proliferation. In addition, transduction with Spred1 shRNA consistently generated significantly more total GFP^+ cells (an additional 63% ± 10.7%) compared with EV control, likely reflecting enhanced cell division (Supplemental Fig. 4). A similar increase in total GFP^+ cells was observed when the electroporation was carried out at E15 and tissue was harvested at E18 (an additional 41.7% ± 4.8% compared with EV control).

We quantified the percentage of dividing cells ($GFP^+/Ki67^+$) in embryos that were electroporated at E15 and harvested at E18. Cortices electroporated with Spred1 shRNAs had significantly more $GFP^+/Ki67^+$ cells compared with EV control vector brains (Spred1 shRNA1 = 24.5% ± 1.2%; Spred1 shRNA2 = 27.8% ± 3.3%; EV control = 15.7% ± 2.6%), consistent with the in vitro data (Fig. 5A,B). Immunohistochemistry for β-tubulin III and GFAP did not reveal any abnormally located neurons or glia in the Spred1 shRNA electroporated brains at this stage (Supplemental Fig. 3C; data not shown).

The observed differences in GFP^+ cell distribution as well as the overall increase in total GFP^+ cell number were not observed when we coelectroporated a Spred1 overexpression construct along with the Spred1 shRNA construct (targeted to the 3′UTR) (Fig. 4A,B), demonstrating that the knockdown phenotype is not an off-target effect. When the Spred1 overexpression plasmid was electroporated into embryos by itself, there were few, if any, $GFP^+/Nestin^+$ cells located in the VZ/SVZ (0.67% ±

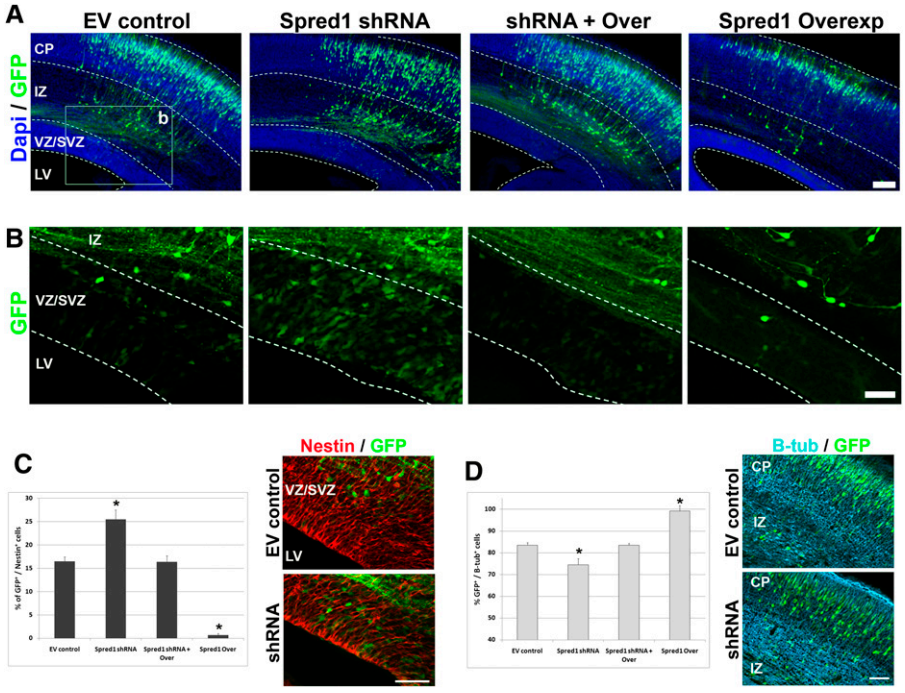

Figure 4. Manipulating the level of Spred1 in vivo impacts the progenitor/neuron compartments. E14 cortices were electroporated with EV control, Spred1 shRNA, Spred1 overexpression, or shRNA and overexpression combined and were analyzed 4 d later. (*A*) Labeling for DAPI and GFP signal in coronal cortical sections. (*B*) Magnified images of the VZ/SVZ regions from *A*. (*C*,*D*) Quantification and representative images of $Nestin^+/GFP^+$ cells within the VZ/SVZ (Nestin/GFP ANOVA, [*] $P < 0.005$, significant Bonferroni post-hoc test) (*C*) and $B\text{-tub}^+/GFP^+$ cells (B-tub/GFP ANOVA, [*] $P < 0.005$, significant Bonferroni post-hoc test) (*D*). (IZ) Intermediate zone; (CP) cortical plate. Bars: *A*,*B*, 100 μm. In *C* and *D*, error bars represent SEM. (EV control, $n = 4$; Spred1 shRNA, $n = 4$; Spred1 shRNA + overexpression, $n = 3$; Spred1 overexpression, $n = 3$).

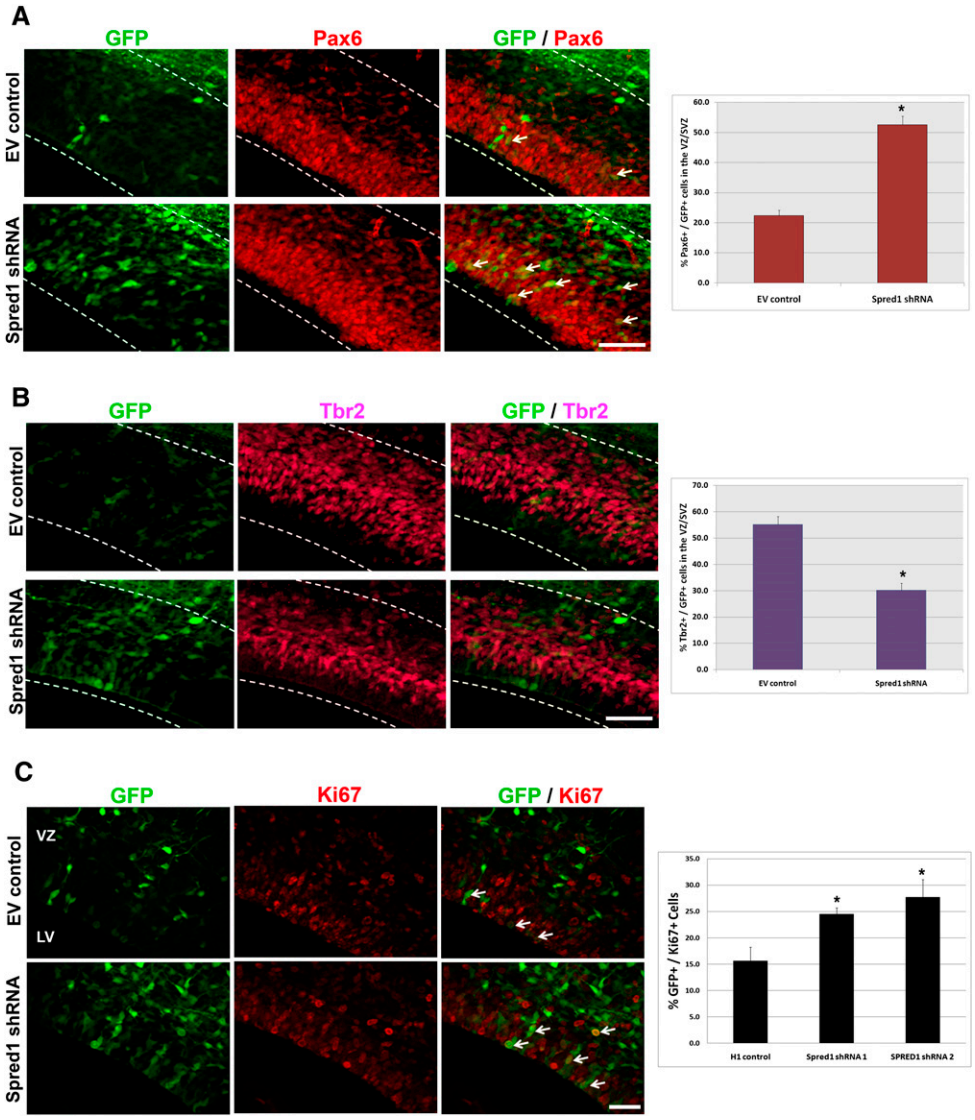

Figure 5. Acute knockdown of Spred1 in cortical progenitors in vivo modulates levels of apical progenitors and increases proliferation. (*A*,*B*) E14 cortices were electroporated at E14 and analyzed 4 d later. (*A*) Sections were stained with Pax6 and quantified for the percentage of Pax6$^+$/GFP$^+$ cells within the VZ/SVZ region (*t*-test, [*] $P < 0.005$). (*B*) Stained with the basal progenitor marker Tbr2 (magenta) and again quantified for Tbr2$^+$/GFP$^+$ cells in the VZ/SVZ region (*t*-test, [*] $P < 0.005$). (EV control, $n = 5$; Spred1 shRNA, $n = 4$). (*C*) E15 cortices were electroporated with EV control or Spred1 shRNA constructs and were analyzed for Ki67$^+$/GFP$^+$ cells 3 d later. (LV) Lateral ventricle; (IZ) intermediate zone; (CP) cortical plate. Bars: *A*–*C*, 50 μm. Error bars represent SEM. (EV control, $n = 6$; Spred1 shRNA1, $n = 8$; Spred1 shRNA2, $n = 4$).

0.4%) after 4 d, as the majority of cells had already migrated out to the cortical plate and were GFP$^+$/β-tubulin$^+$ (99.3% ± 0.4%) by E18 (Fig. 4A–D), consistent with the premature neuronal differentiation observed in vitro. The fact that overexpression and reduced expression of Spred1 in vivo produce essentially opposite phenotypes demonstrates the functional importance of precisely regulating Spred1 levels.

Embryonic Spred1 knockdown leads to PVH

Since acute knockdown of Spred1 levels in vivo via in utero electroporation led to an increase in embryonic progenitor proliferation, we investigated whether this would result in changes in the cortical architecture in postnatal animals. After electroporation at E15, animals were sacrificed 13 d later at postnatal day 7 (P7). The majority of EV control GFP$^+$-transfected cells had migrated out to the cortical plate, contributing cells to the upper layers of the cortex (layers 2 and 3) with elaborated apical dendrites and axonal processes. A few cells in the cortical plate were also GFAP$^+$ astrocytes. In the remainder of the germinal zone, a few GFP$^+$ cells were retained in the SVZ, and most were GFAP$^+$ (Fig. 6A; data not shown). Cortices electroporated with Spred1 shRNA displayed a similar pattern of GFP expression in the upper

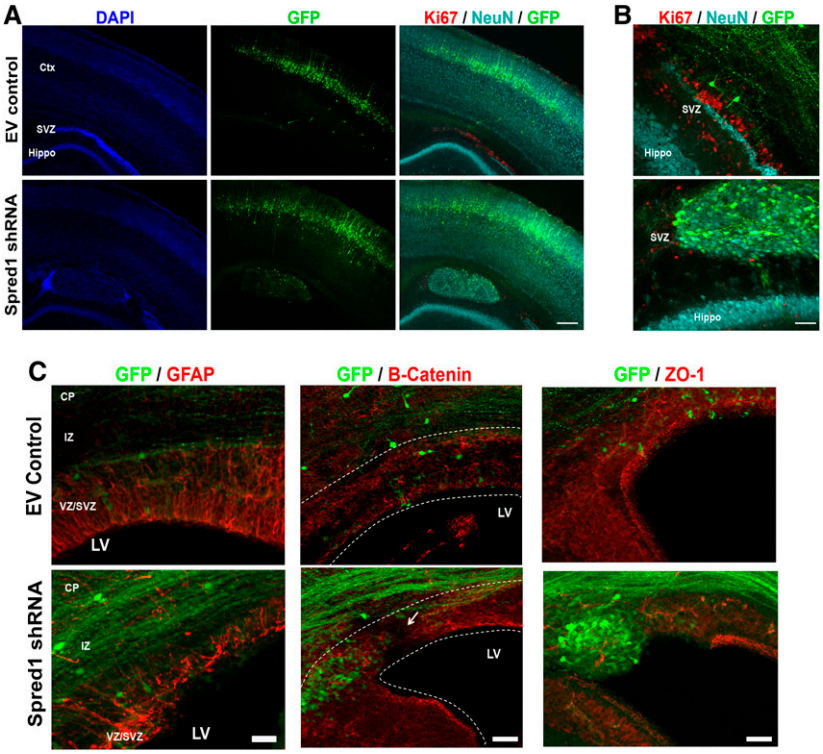

Figure 6. Acute knockdown of Spred1 in cortical progenitors in vivo leads to PVH. E15 cortices were electroporated with EV control or Spred1 shRNA constructs and were analyzed at P7 (*A*,*B*), P0 (*C*, *left* and *middle* panels), or P2 (*C*, *right* panel). (*A*) P7 cortices immunolabeled for DAPI (*left* panel, blue), GFP (*middle* panel, green), and triple labeling (*right* panel) for Ki67 (red), NeuN (light blue), and GFP (green). Fifty-four percent of Spred1 shRNA cortices exhibited GFP$^+$ cell masses next to or near the SVZ (n = 12). None were observed in EV control cortices (n = 10). (*B*) Higher magnification of SVZ region showing GFP$^+$ cells. (*C*, *left* panels) P0 and P2 cortices immunolabeled for GFP (green) and GFAP (red); note the disrupted, nonradial orientation of the GFAP$^+$ cells after Spred1 shRNA treatment. (*Middle*) β-Catenin (red); the arrow denotes a region of weak β-catenin signal. (*Right* panels) ZO-1 (red); note the loss of ZO-1 expression by P2 in regions that have GFP$^+$ cells next to the ventricle in Spred1 shRNA conditions. (Hippo) Hippocampus; (Ctx) cortex; (LV) lateral ventricle; (IZ) intermediate zone; (CP) cortical plate. Bars: *A*, 200 μm *B*,*C*, 50 μm.

cortical layers, and quantification revealed no significant differences in the number of GFP$^+$ cells in the cortical plate (Fig. 6A; Supplemental Fig. 6). However, in ~60% of embryos, there was a mass of GFP$^+$ cells just above or within the SVZ (Fig. 6A,B). The cellular masses varied in size from 50 to 400 μm, and consisted mostly of NeuN$^+$ neurons and GFAP$^+$ astrocytes (Fig. 6B; Supplemental Fig. 7C,D). They included a small number (<2%) of Ki67$^+$ proliferating cells, and were vascularized, revealed by CD31 staining (Fig. 6B; Supplemental Fig. 7B). These heterotopia were never observed when we electroporated the EV control plasmid, or a shRNA construct targeting a related protein, Sprouty2 (Supplemental Fig. 9).

To address the origin of these periventricular masses, we analyzed the cytoarchitecture of Spred1 shRNA electroporated cortices harvested at intermediate time points: P0 and P2 (6 and 8 d post-electroporation). While the majority of GFP$^+$ cells should have migrated out to the cortical plate at these time points, as seen in the EV control brains, Spred1 shRNA animals retained many GFP$^+$ cells in the germinal zones. The organization of the VZ/SVZ appeared disrupted after Spred1 shRNA treatment, and staining with β-catenin, ZO-1, and N-cadherin was significantly reduced in the transduced area, indicating alterations in junctional integrity and in the neuroepithelial organization (Fig. 6C; Supplemental Fig. 8). Moreover, after Spred1 shRNA treatment, apical radial glial processes (GFAP$^+$ at this stage) were no longer clearly oriented and organized, as they were in controls (Fig. 6C), Thus, Spred1 knockdown, while not impairing early neuronal migration, eventually leads to disrupted germinal zone and radial glial guidance structures, which are likely to be important factors in disrupting late migration and forming the periventricular masses.

Discussion

In this study, we examined the expression and function of Spred1, a recently discovered negative regulator of Ras–MAPK–ERK, during development of the cerebral cortex. We provide evidence that Spred1 is expressed strongly and rather specifically in embryonic CNS germinal zones, and is rapidly down-regulated upon neuronal differentiation. Perturbation in Spred1 levels in either direction has a significant effect on the progenitor cell self-renewal/differentiation decision, leading to profound changes in production of cortical cells. Our data indicate that Spred1 is a key cell-intrinsic modulator of NSC proliferation, and especially of Pax6$^+$ apical progenitors, which include radial glial (Englund et al. 2005) that play essential roles in cell genesis and cytoarchitecture formation.

During forebrain development, NSCs and progenitor cells that reside in the VZ and SVZ undergo a delicate balance of symmetric and asymmetric divisions to produce the appropriate numbers of neurons and glia needed to build the mature tissue. The progenitor cells receive information from a variety of sources, and growth factors and cytokines influence their behavior by modulating the balance of signaling pathways such as Ras–MAPK–ERK and gp130–Jak–Stat. These signaling pathways are internally regulated by adaptor and effector proteins that promote or dampen activation at different levels of the cascade. The ability of these proteins to modulate one or multiple pathways and to intervene at different points in

a pathway allows them to influence different aspects of progenitor cell behavior. Thus, by using a variety of modulators and effectors, output of germinal zones can be precisely regulated.

Prior studies showed that Spred1 can specifically modulate Ras–MAPK–ERK (Wakioka et al. 2001; Nonami et al. 2004) and is expressed in the embryonic and adult mouse brain (Engelhardt et al. 2004). More recently, mutations in Spred1 have been associated with an NF-1-like disorder in humans (Brems et al. 2007). Here, we demonstrate that Spred1 is highly expressed throughout development in mouse CNS germinal zones, but that it negatively regulates self-renewal and proliferation of the apical $Pax6^+$ radial glial progenitors but not the more basal $Tbr2^+$ progenitors. It will be interesting to examine the molecular targets of Spred1 in radial glia versus basal progenitor cells, as this could reveal significant differences in cell division control in these two progenitor classes.

Even though knockdown of Spred1 is heritable by virtue of lentiviral delivery in vitro, NSCs and progenitor cells that were transduced do not continue to divide out of control, but eventually differentiate. Thus, other mechanisms are able to circumvent this perturbation in the Ras–MAPK–ERK signaling pathway. This could explain why most patients deficient in Spred1 activity can have largely normal nervous system development, while still exhibiting some structural changes that are associated with neurological and mental impairments. Progenitor cells treated with Spred1 shRNA differentiated into apparently morphologically normal neurons and astrocytes when either growth factor-starved or induced with CNTF. This is most likely because Spred1 appears to influence largely the Ras–MAPK–ERK pathway, and does not interact with the gp130–JAK–STAT pathway (Inoue et al. 2005). While Spred1 does not appear to contribute to timing the onset of glial differentiation, it remains possible that it could play a role in glia progenitor proliferation, as it is still expressed in progenitor cells at late stages of embryonic development.

Using in utero electroporation, we characterized the function of Spred1 in vivo in the developing cortex. Knockdown of Spred1 at midgestation stimulated progenitor proliferation, and many of the electroporated embryos displayed PVH of various sizes by early postnatal stages. The heterotopia consisted entirely of GFP^+ cells, which indicates they formed cell-autonomously. PVH are relatively common developmental anomalies that are frequently linked to epilepsy and, in some cases, to mental retardation. They are characterized as largely neuronal masses next to or lining the ventricle, while in these patients the gross structure of the overlying cortex, the cortical lamination, is typically relatively unaffected. Our findings are similar, as we see that, after Spred1 knockdown, most neurons migrate normally into the cortical plate, but PVH are found in early postnatal stages in more than half of the transduced animals.

The mechanism of PVH formation was originally seen as a defect in neuronal migration. However, more recently, it has become apparent that mutations in genes affecting vesicular trafficking and maintenance of the neuroependymal lining can be causal. These mutations lead to disruption of the ventricular surface and radial glial end feet that in turn contribute to migration defects (Sarkisian et al. 2006; Ferland et al. 2009). Mutations in *Filamin A*, a regulator of the actin cytoskeleton that is associated with vesicular movement in the transgolgi, is a common cause of PVH, and mutations in *MEKK4*, a Filamin A regulator, also can underlie this disorder (Liu et al. 1997; Sarkisian et al. 2006). Alterations in *Arfgef2* and *Napa*, important for vesicular trafficking and fusion, lead to progressive loss of cell adhesion and neuroependymal integrity resulting in PVH (Ferland et al. 2009). Spred1 is a multidomain scaffolding protein, and it contains an Ena/VASP domain that can modulate actin stress fiber remodeling through its ability to interact with the Rho–Rock signaling pathway. Moreover, we show here that Spred1 is associated with specific endosome vesicles, which raises the intriguing possibility that it has a role in vesicular trafficking, like the other previously characterized PVH genes. Future studies on the detailed mechanism of this process—for example, whether Spred1 interacts with MEKK4/Filamin A, or impacts actin cytoskeleton assembly or the vesicular trafficking network—will be worthwhile.

While these findings have focused on reduction of endogenous Spred1, we note that overexpression of Spred1 causes premature neuronal differentiation, and that some of the neurons generated had abnormal morphology (data not shown). We know that hypoactive Ras–MAPK–ERK can lead to microcephaly in the case of RSK2 mutations associated with Coffin-Lowry syndrome (Trivier et al. 1996), or decreased NSC proliferation with *Erk2* deletion in mice (Samuels et al. 2008). Thus, we conclude that precise regulation of the levels of Spred1 will be important throughout development to ensure normal CNS development.

In conclusion, this study introduces Spred1 as a functionally significant modulator of the Ras pathway that affects NSC self-renewal and progenitor proliferation, and has an important role in VZ/SVZ organization. Understanding the function and regulation of Spred1 in this context can help shed light on its role as a putative tumor suppressor and possible modulator of the vesicular trafficking network, and lead to a greater understanding of how Spred1 mutations and Ras–MAPK–ERK modulation cause CNS abnormalities.

Materials and methods

Cortical cell culture

For adherent cultures, cerebral cortices of timed pregnant Swiss Webster mouse embryos (Taconic Farms) were dissociated and cultured as described previously in serum-free DMEM medium with 10 ng/mL FGF2 (Invitrogen) in PLL-coated Terasaki plates (Qian et al. 1998). For clonal analysis, 10–20 cells were plated in Terasaki plate microwells, and clonal development was monitored by daily microscopic inspection. In some cultures, 10 ng/mL CNTF (R&D Systems) was added at 3 and 5 DIV.

For neurosphere cultures, single dissociated cortical cells were cultured in serum-free DMEM medium with 20 ng/mL FGF2 and EGF (Invitrogen) in ultralow binding six-well plates (CoStar/Corning) for 7 DIV. To subclone, neurospheres were collected and gently dissociated using papain (Worthington) for 20 min at 37°C with gentle agitation. Cells were replated at equal density for each condition, and the number of neurospheres generated was counted after 7 DIV.

For transfection experiments, cortical progenitors were plated as adherent cultures in six-well plates in media conditions listed above. Twelve hours after plating, cells were transfected with either EV control, Spred1 shRNA, or Spred1 overexpression plasmids using Stemfect 2.0 (Stemgent). Twelve micrograms of plasmid and 2 μL of Stemfect were used per well. Fifteen random fields per condition were imaged and counted in each experiment.

In situ hybridization

In situ hybridization was carried out as described previously (Abramova et al. 2005). Briefly, an ~600-base-pair (bp) region of Spred1 cDNA was cloned and sequence-verified into TA TOPO sequencing vector (Invitrogen). Antisense and sense digoxygen (DIG)-labeled probes were synthesized using T7 and T3 polymerase, and probes were quantified using DIG RNA probe standards (Roche). Spred1 in situ primers were as follows: Forward, 5′-ATGACTCAAGTGGTGGATGGCT-3′; and Reverse, 5′-TTGGGACTTTAGGCTCCCACAT-3′.

Immunostaining

Cryostat sections and cell cultures were fixed and immunostained as described previously (Shen et al. 2006). Primary antibodies used were as follows: β-tubulin III, mouse IgG2b, 1:400 (Sigma); GFAP, rabbit IgG, 1:400 (Dako); Ki67, rabbit IgG, 1:1000 (Lab Visions); Pax6, mouse IgG1, 1:200 (Developmental Studies Hybridoma Bank); N-cadherin, mouse IgG, 1:200 (BD Biosciences); Nestin, mouse IgG1, 1:25 (Developmental Studies Hybridoma Bank); NeuN, mouse IgG1, 1:100 (Chemicon); CD31, rat IgG, 1:200 (BD Biosciences); Rab5, mouse IgG1, 1:200 (BD Biosciences); Rab11, mouse IgG2b, 1:200 (BD Biosciences); Spred1, rabbit IgG, 1:100 (generous gift from Dr. Kai Schuh); Tbr2, rabbit IgG, 1:250 (Chemicon); ZO-1, rabbit IgG (Invitrogen). Immunoreactivity was visualized using Alexa Fluor-conjugated secondary antibodies (1:1000; Molecular Probes). Phase and fluorescent images were acquired using a Zeiss Z-1 apotome inverted microscope and a Zeiss AxioCam MRm digital camera with Axiovision 4.6 software. Figures and images were assembled using Adobe Photoshop.

Western blots

Cell culture or tissue protein was isolated with M-Per or T-Per, respectively, containing HALT protease inhibitors (Thermo Scientific) and Phospho-Stop phosphatase inhibitors (Roche), and protein concentration was calculated using the BCA assay. Equal amounts of protein were loaded onto 10% NuPAGE Novex Bis-Tris gels (Invitrogen) and were transferred onto nitrocellulose membranes. Membranes were blocked in 5% BSA for 1 h and then probed with primary antibody overnight at 4°C. Spred1, rabbit IgG, 1:500 (Dr. Kai Schuh); p-ERK, rabbit IgG, 1:500 (Cell Signaling); ERK2 rabbit IgG, 1:5000 (Cell Signaling); total ERK Rabbit IgG, 1:5000 (Cell Signaling); p-AKT, rabbit IgG, 1:1000 (Cell Signaling); GAPDH rabbit IgG, 1:1000 (Cell Signaling); Sprouty1, rabbit IgG, 1:500 (Invitrogen); and Sprouty2, rabbit IgG, 1:1000 (Santa Cruz Biotechnologies) were used. Peroxidase-conjugated secondary antibodies (Jackson ImmunoResearch) were used at 1:10,000 for 1 h at room temperature. Supersignal West Pico (Thermo Scientific) was used as the chemical substrate, and blots were visualized on Bio-Rad XRS GelDock using Quantity One software.

Lentivial vector production and viral packaging

shRNA and overexpression constructs for Spred1, Sprouty1, and Sprouty2 were constructed, harvested, and titered as described previously (Shen et al. 2006; Fasano et al. 2007). Oligonucleotides containing a 19mer targeting either the ORF or 3′UTR, followed by a loop sequence and then reverse complement, were synthesized and cloned into the H1 lentiviral vector using XbaI/SmaI. The 19mer sequences are as follows: Spred1 shRNA1, 5′-CG GCAAATATCTAAGGAAT-3′; Spred1 shRNA2, 5′-AGAATA AATCCTCGAGATA-3′; Spred1 shRNA3, 5′-CTGGATAGTT AGTGTGAAA-3′; Sprouty2 shRNA, 5′-GCCGGGTTGTCGT TGTAAA-3′. For overexpression constructs, the ORF of each gene was PCR-amplified, sequence-verified, and cloned into a modified version of FUGW. An IRES-eGFP was also included for visualization in cells. For viral transduction, lentiviral vectors were added to dissociated cortical cultures just before plating at a multiplicity of infection of 10.

In utero electroporation

Plasmids were transfected by in utero electroporation as described previously (Fasano et al. 2007). The lateral ventricle of E14 or E15 timed pregnant Swiss Webster embryos were microinjected (Nanojet, Drummond Scientific) with 1 μL of plasmid (Endotoxin-free, 2.0 μg/μL; Qiagen) mixed with Fast green (2 mg/mL; Sigma) as a tracer. The square electroporator (BTX) was used to deliver five 50-ms pulses of 50 V with 950-ms intervals. Dissected brains were fixed in 4% paraformadehyde overnight at 4°C, cryoprotected in 30% sucrose, and then cryosectioned (Leica) coronally at 40 μm as floating sections. Sections were then imaged on a Zeiss Z1 apotome inverted microscope. For analysis, two to four sections from each embryo were used to calculate the average GFP^+ cells in each condition. Three to eight embryos were used to calculate final averages.

Statistics

All statistical tests, *t*-tests, and one-way ANOVAs with Bonferroni post-hoc tests were performed with Statistica version 7.0.

Acknowledgments

We thank Kai Schuh (University of Wuerzburg) for the generous gift of Spred1 antibody. This work was supported by NIH grant numbers R37 NS033529 (to S.T.) and F31 NS059107-01 (to T.N.P.). T.N.P. conceived the project, conducted the experiments, and wrote the manuscript. S.T. supervised the project, data collection analysis, and manuscript editing.

References

Abramova N, Charniga C, Goderie SK, Temple S. 2005. Stage-specific changes in gene expression in acutely isolated mouse CNS progenitor cells. *Dev Biol* **283:** 269–281.

Balestri P, Vivarelli R, Grosso S, Santori L, Farnetani MA, Galluzzi P, Vatti GP, Calabrese F, Morgese G. 2003. Malformations of cortical development in neurofibromatosis type 1. *Neurology* **61:** 1799–1801.

Barnabe-Heider F, Miller FD. 2003. Endogenously produced neurotrophins regulate survival and differentiation of cortical

progenitors via distinct signaling pathways. *J Neurosci* **23:** 5149–5160.

Barnabe-Heider F, Wasylnka JA, Fernandes KJ, Porsche C, Sendtner M, Kaplan DR, Miller FD. 2005. Evidence that embryonic neurons regulate the onset of cortical gliogenesis via cardiotrophin-1. *Neuron* **48:** 253–265.

Bayer SA, Altman J, Russo RJ, Dai XF, Simmons JA. 1991. Cell migration in the rat embryonic neocortex. *J Comp Neurol* **307:** 499–516.

Brems H, Chmara M, Sahbatou M, Denayer E, Taniguchi K, Kato R, Somers R, Messiaen L, De Schepper S, Fryns JP, et al. 2007. Germline loss-of-function mutations in SPRED1 cause a neurofibromatosis 1-like phenotype. *Nat Genet* **39:** 1120–1126.

Bundschu K, Walter U, Schuh K. 2007. Getting a first clue about SPRED functions. *Bioessays* **29:** 897–907.

Burrows RC, Wancio D, Levitt P, Lillien L. 1997. Response diversity and the timing of progenitor cell maturation are regulated by developmental changes in EGFR expression in the cortex. *Neuron* **19:** 251–267.

Cichowski K, Jacks T. 2001. NF1 tumor suppressor gene function: Narrowing the GAP. *Cell* **104:** 593–604.

Costa RM, Federov NB, Kogan JH, Murphy GG, Stern J, Ohno M, Kucherlapati R, Jacks T, Silva AJ. 2002. Mechanism for the learning deficits in a mouse model of neurofibromatosis type 1. *Nature* **415:** 526–530.

Cui Y, Costa RM, Murphy GG, Elgersma Y, Zhu Y, Gutmann DH, Parada LF, Mody I, Silva AJ. 2008. Neurofibromin regulation of ERK signaling modulates GABA release and learning. *Cell* **135:** 549–560.

Dasgupta B, Gutmann DH. 2005. Neurofibromin regulates neural stem cell proliferation, survival, and astroglial differentiation in vitro and in vivo. *J Neurosci* **25:** 5584–5594.

Denayer E, Ahmed T, Brems H, Van Woerden G, Borgesius NZ, Callaerts-Vegh Z, Yoshimura A, Hartmann D, Elgersma Y, D'Hooge R, et al. 2008. Spred1 is required for synaptic plasticity and hippocampus-dependent learning. *J Neurosci* **28:** 14443–14449.

Engelhardt CM, Bundschu K, Messerschmitt M, Renne T, Walter U, Reinhard M, Schuh K. 2004. Expression and subcellular localization of Spred proteins in mouse and human tissues. *Histochem Cell Biol* **122:** 527–538.

Englund C, Fink A, Lau C, Pham D, Daza R, Bulfone A, Kowalczyk T, Hevner RF. 2005. Pax6, Tbr2, and Tbr1 are expressed sequentially by radial glia, intermediate progenitor cells, and postmitotic neurons in the developing neocortex. *J Neurosci* **25:** 247–251.

Fasano CA, Dimos JT, Ivanova NB, Lowry N, Lemischka IR, Temple S. 2007. shRNA knockdown of Bmi-1 reveals a critical role for p21–Rb pathway in NSC self-renewal during development. *Cell Stem Cell* **1:** 87–99.

Fedi M, Anne Mitchell L, Kalnins RM, Gutmann DH, Perry A, Newton M, Brodtmann A, Berkovic SF. 2004. Glioneuronal tumours in neurofibromatosis type 1: MRI-pathological study. *J Clin Neurosci* **11:** 745–747.

Ferland RJ, Batiz LF, Neal J, Lian G, Bundock E, Lu J, Hsiao YC, Diamond R, Mei D, Banham AH, et al. 2009. Disruption of neural progenitors along the ventricular and subventricular zones in periventricular heterotopia. *Hum Mol Genet* **18:** 497–516.

Gauthier AS, Furstoss O, Araki T, Chan R, Neel BG, Kaplan DR, Miller FD. 2007. Control of CNS cell-fate decisions by SHP-2 and its dysregulation in Noonan syndrome. *Neuron* **54:** 245–262.

Goh KL, Cai L, Cepko CL, Gertler FB. 2002. Ena/VASP proteins regulate cortical neuronal positioning. *Curr Biol* **2:** 565–569.

Hegedus B, Dasgupta B, Shin JE, Emnett RJ, Hart-Mahon EK, Elghazi L, Bernal-Mizrachi E, Gutmann DH. 2007. Neurofibromatosis-1 regulates neuronal and glial cell differentiation from neuroglial progenitors in vivo by both cAMP- and Ras-dependent mechanisms. *Cell Stem Cell* **1:** 443–457.

Inoue H, Kato R, Fukuyama S, Nonami A, Taniguchi K, Matsumoto K, Nakano T, Tsuda M, Matsumura M, Kubo M, et al. 2005. Spred-1 negatively regulates allergen-induced airway eosinophilia and hyperresponsiveness. *J Exp Med* **201:** 73–82.

Jin K, Zhu Y, Sun Y, Mao XO, Xie L, Greenberg DA. 2002. Vascular endothelial growth factor (VEGF) stimulates neurogenesis in vitro and in vivo. *Proc Natl Acad Sci* **99:** 11946–11950.

Kato R, Nonami A, Taketomi T, Wakioka T, Kuroiwa A, Matsuda Y, Yoshimura A. 2003. Molecular cloning of mammalian Spred-3 which suppresses tyrosine kinase-mediated Erk activation. *Biochem Biophys Res Commun* **302:** 767–772.

Korf BR, Schneider G, Poussaint TY. 1999. Structural anomalies revealed by neuroimaging studies in the brains of patients with neurofibromatosis type 1 and large deletions. *Genet Med* **1:** 136–140.

Lawrence DW, Comerford KM, Colgan SP. 2002. Role of VASP in reestablishment of epithelial tight junction assembly after Ca^{2+} switch. *Am J Cell Physiol* **282:** 1235–1245.

Liu G, Thomas L, Warren RA, Enns CA, Cunningham CC, Harwig JH, Thomas G. 1997. Cytoskeletal protein ABP-280 directs the intracellular trafficking of furin and modulates proprotein processing in the endocytic pathway. *J Cell Biol* **139:** 1719–1733.

Lush ME, Li Y, Kwon CH, Chen J, Parada LF. 2008. Neurofibromin is required for barrel formation in the mouse somatosensory cortex. *J Neurosci* **28:** 1580–1587.

Marui T, Hashimoto O, Nanba E, Kato C, Tochigi M, Umekage T, Ishijima M, Kohda K, Kato N, Sasaki T. 2004. Association between the neurofibromatosis-1 (NF1) locus and autism in the Japanese population. *Am J Med Genet B Neuropsychiatr Genet* **131B:** 43–47.

Mbarek O, Marouillat S, Martineau J, Barthelemy C, Muh JP, Andres C. 1999. Association study of the NF1 gene and autistic disorder. *Am J Med Genet* **88:** 729–732.

Miller FD, Gauthier AS. 2007. Timing is everything: Making neurons versus glia in the developing cortex. *Neuron* **54:** 357–369.

Miyoshi K, Wakioka T, Nishinakamura H, Kamio M, Yang L, Inoue M, Hasegawa M, Yonemitsu Y, Komiya S, Yoshimura A. 2004. The Sprouty-related protein, Spred, inhibits cell motility, metastasis, and Rho-mediated actin reorganization. *Oncogene* **23:** 5567–5576.

Nonami A, Kato R, Taniguchi K, Yoshiga D, Taketomi T, Fukuyama S, Harada M, Sasaki A, Yoshimura A. 2004. Spred-1 negatively regulates interleukin-3-mediated ERK/mitogen-activated protein (MAP) kinase activation in hematopoietic cells. *J Biol Chem* **279:** 52543–52551.

Noonan JA. 1994. Noonan syndrome. An update and review for the primary pediatrician. *Clin Pediatr (Phila)* **33:** 548–555.

Qian X, Goderie SK, Shen Q, Stern JH, Temple S. 1998. Intrinsic programs of patterned cell lineages in isolated vertebrate CNS ventricular zone cells. *Development* **125:** 3143–3152.

Samuels IS, Karlo JC, Faruzzi AN, Pickering K, Herrup K, Sweatt JD, Saitta SC, Landreth GE. 2008. Deletion of ERK2 mitogen-activated protein kinase identifies its key roles in cortical neurogenesis and cognitive function. *J Neurosci* **28:** 6983–6995.

Sarkisian MR, Bartley CM, Chi H, Nakamura F, Hashimoto-Torii K, Torii M, Flavell RA, Rakic P. 2006. MEKK4 signaling regulates filamin expression and neuronal migration. *Neuron* **52:** 789–801.

Sasaki A, Taketomi T, Kato R, Saeki K, Nonami A, Sasaki M, Kuriyama M, Saito N, Shibuya M, Yoshimura A. 2003. Mammalian Sprouty4 suppresses Ras-independent ERK activation by binding to Raf1. *Nat Cell Biol* **5:** 427–432.

Schubbert S, Shannon K, Bollag G. 2007. Hyperactive Ras in developmental disorders and cancer. *Nat Rev Cancer* **7:** 295–308.

Shen Q, Wang Y, Dimos JT, Fasano CA, Phoenix TN, Lemischka IR, Ivanova NB, Stifani S, Morrisey EE, Temple S. 2006. The timing of cortical neurogenesis is encoded within lineages of individual progenitor cells. *Nat Neurosci* **9:** 743–751.

Trivier E, De Cesare D, Jacquot S, Pannetier S, Zackai E, Young I, Mandel JL, Sassone-Corsi P, Hanauer A. 1996. Mutations in the kinase Rsk-2 associated with Coffin-Lowry syndrome. *Nature* **384:** 567–570.

Vaccarino FM, Schwartz ML, Raballo R, Nilsen J, Rhee J, Zhou M, Doetschman T, Coffin JD, Wyland JJ, Hung YT. 1999. Changes in cerebral cortex size are governed by fibroblast growth factor during embryogenesis. *Nat Neurosci* **2:** 848. doi: 10.1038/12226.

Vivarelli R, Grosso S, Calabrese F, Farnetani M, Di Bartolo R, Morgese G, Balestri P. 2003. Epilepsy in neurofibromatosis 1. *J Child Neurol* **18:** 338–342.

Wakioka T, Sasaki A, Kato R, Shouda T, Matsumoto A, Miyoshi K, Tsuneoka M, Komiya S, Baron R, Yoshimura A. 2001. Spred is a Sprouty-related suppressor of Ras signalling. *Nature* **412:** 647–651.

Zhu Y, Parada LF. 2001. Neurofibromin, a tumor suppressor in the nervous system. *Exp Cell Res* **264:** 19–28.

Zhu Y, Romero MI, Ghosh P, Ye Z, Charnay P, Rushing EJ, Marth JD, Parada LF. 2001. Ablation of NF1 function in neurons induces abnormal development of cerebral cortex and reactive gliosis in the brain. *Genes & Dev* **15:** 859–876.

Zhu Y, Harada T, Liu L, Lush ME, Guignard F, Harada C, Burns DK, Bajenaru ML, Gutmann DH, Parada LF. 2005. Inactivation of NF1 in CNS causes increased glial progenitor proliferation and optic glioma formation. *Development* **132:** 5577–5588.